Electronic Structure of Carbonyl Oxides: Semiempirical Calculations of Ground-State Properties and UV–Vis Spectra

Dieter Cremer,* Thomas Schmidt, Wolfram Sander,* and Peter Bischof

Institut für Organische Chemie, Universität Köln, Greinstr. 4, D-5000 Köln 41, West Germany, and Organisch-Chemisches Institut der Universität Heidelberg, Im Neuenheimer Feld 270, D-6900 Heidelberg, West Germany

Received September 6, 1988

Semiempirical calculations have been carried out on a variety of substituted carbonyl oxides employing the MINDO/3-UHF method, which provides a reasonable description of ground-state properties of carbonyl oxides. The effects of π-acceptor and π-donor substituents have been found to lead to typical changes in the heavy-atom geometry and in the charge distribution. Calculations suggest that strong π-donors entail zwitterionic character of carbonyl oxide while weak π-donors and π-acceptors hardly change the biradical character of the parent compound. Predictions with regard to the nucleophilicity of carbonyl oxides can be made from calculations. CNDO/S calculations on the electronic transitions of carbonyl oxides are in excellent agreement with the spectroscopic data available from matrix isolation experiments and laser flash photolysis studies. The influence of substituents on the UV–vis spectra of carbonyl oxides is discussed.

Introduction

Carbonyl oxides are important reactive intermediates in oxidation reactions of carbenes and diazo compounds and in the ozonolysis of olefins. In the last few years, direct spectroscopic evidence for these elusive species has appeared in the literature (see Table I and Scheme I).[1-6] The most important techniques for a direct spectroscopic characterization of carbonyl oxides have been matrix isolation[1-3] and laser flash photolysis.[4-6] While time-resolved spectroscopy can be carried out at room temperature in organic solvents (Table I), the only structural information obtained by this technique stems from the absorption spectra of low resolution in the UV–vis region.[4-6] Matrix isolation, on the other hand, leads to well-resolved UV–vis and IR spectra of carbonyl oxides, but is limited to rather exotic reaction conditions (cryogenic temperatures, solid inert gas as solvent).[1-3]

Simultaneously with the increasing number of experimental studies, several theoretical papers on the electronic structure of carbonyl oxides have been published.[7-12]

Scheme I

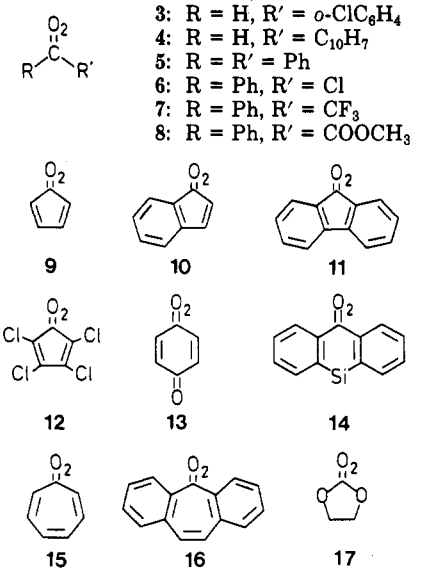

Rigorous ab initio investigations demonstrated that the inclusion of correlation corrections into the quantum chemical method employed is essential for a reliable description of the electronic nature of carbonyl oxides.[7-10] Møller-Plesset second-order (MP2) and fourth-order (MP4) calculations,[8] configuration-interaction (CI) calculations,[7,10] and multiconfigurational SCF (MCSCF) calculations[10] unanimously describe the ground state of carbonyl oxide **1** to be closer to a singlet biradical rather than a zwitterion (compare with resonance structures a and b–f in Scheme II).

Because of the large computational effort required for an ab initio description of carbonyl oxides, these calculations have been restricted to the parent compound **1** or to simply substituted derivatives. Semiempirical calculations, which also can handle substituted carbonyl oxides of experimental interest, seem to yield conflicting results. For example, a MINDO/3 CI investigation carried out on **1**[11] leads to a description of its electronic structure that is in line with the ab initio results. However, a restricted HF (RHF) MINDO/3 study predicts significant zwitterionic character for **1** and phenyl-substituted carbonyl oxide (**2**).[12]

(1) (a) Bell, G. A.; Dunkin, I. R. *J. Chem. Soc., Chem. Commun.* **1983**, 1213. (b) Dunkin, I. R.; Shields, C. J. *J. Chem. Soc., Chem. Commun.* **1986**, 154. (c) Bell, G. A.; Dunkin, I. R.; Shields, C. J. *Spectrochim. Acta* **1985**, *41A*, 1221.

(2) (a) Sander, W. *Angew. Chem.* **1986**, *98*, 255; *Angew. Chem., Int. Ed. Engl.* **1986**, *25*, 255. (b) Sander, W. *Spectrochim. Acta* **1987**, *43A*, 637. (c) Sander, W. *J. Org. Chem.* **1988**, *53*, 125. (d) Sander, W. *J. Org. Chem.* **1988**, *53*, 2091. (e) Sander, W. *J. Org. Chem.* **1989**, *54*, 333.

(3) Ganzer, G. A.; Sheridan, R. S.; Liu, M. T. H. *J. Am. Chem. Soc.* **1986**, *108*, 1517.

(4) Sugawara, T.; Iwamura, H.; Hayashi, H.; Sekiguchi, A.; Ando, W.; Liu, M. T. H. *Chem. Lett.* **1983**, 1261.

(5) (a) Werstiuk, N. H.; Casal, H. L.; Scaiano, J. C. *Can. J. Chem.* **1984**, *62*, 2391. (b) Casal, H. L.; Tanner, M.; Werstiuk, N. H.; Scaiano, J. C. *J. Am. Chem. Soc.* **1985**, *107*, 4616. (c) Barcus, R. L.; Hadel, L. M.; Johnston, L. J.; Platz, M. S.; Savino, T. G.; Scaiano, J. C. *J. Am. Chem. Soc.* **1986**, *108*, 3928.

(6) Fujiwara, Y.; Tanimoto, Y.; Itoh, M.; Hirai, K.; Tomioka, H. *J. Am. Chem. Soc.* **1987**, *109*, 1942.

(7) Harding, L. B.; Goddard, W. A. *J. Am. Chem. Soc.* **1978**, *100*, 7180.

(8) (a) Cremer, D. *J. Am. Chem. Soc.* **1979**, *101*, 7199. (b) Gauss, J.; Cremer, D. *Chem. Phys. Lett.* **1987**, *133*, 420. (c) Cremer, D.; Schmidt, T.; Gauss, J.; Radhakrishnan, T. P. *Angew. Chem.* **1988**, 100, 431; *Angew. Chem., Int. Ed. Engl.* **1988**, *27*, 427. (d) Cremer, D.; Schindler, M. *Chem Phys. Lett.* **1987**, *133*, 293. (e) Cremer, D. *J. Am. Chem. Soc.* **1981**, *103*, 3619, 3627, 3633.

(9) (a) Yamaguchi, K.; Yabushita, S.; Fueno, T. *Chem. Phys. Lett.* **1980**, *71*, 563. (b) Yamaguchi, K.; Ohta, K.; Yabushita, S.; Fueno, T. *J. Chem. Phys.* **1978**, *68*, 4323.

(10) Karlström, G.; Engström, G.; Jönsson, B. *Chem. Phys. Lett.* **1979**, *67*, 343.

(11) Hull, L. A. *J. Org. Chem.* **1978**, *43*, 2780.

(12) Sawaki, Y.; Kato, H.; Ogata, Y. *J. Am. Chem. Soc.* **1981**, *103*, 3832.

0022-3263/89/1954-2515$01.50/0

Table I. UV-Vis Spectroscopic Data of Some Carbonyl Oxides RR'COO

carbonyl oxide[a]	matrix isolation[b]	laser flash photolysis[c]	lit.
2, R = H, R' = Ph	Ar, 398 nm		21
3, R = H, R' = *o*-ClC_6H_4	Ar, 406 nm		2b
4, R = H, R' = $C_{10}H_7$		cyclohexane, 435 nm	5c
5, R = R' = Ph	Ar, 422 nm	CH_3CN, 410 nm	2a, 5a
6, R = Ph, R' = Cl	Ar, 400 nm		3
7, R = Ph, R' = CF_3	Ar, 378 nm		2c
8, R = Ph, R' = $COOCH_3$		Freon, 410 nm	6
9	N_2, 420 nm		1c
10	N_2, 445 nm		1c
11	N_2, 460 nm	Freon, 450 nm	1c, 5b
12	N_2, 395 nm		1c
13	Ar, 462 nm		2d
14		cyclohexane, 425 nm	4

[a] Substituents are denoted by R and R' when the position (syn or anti) is not known. [b] Spectra taken at 10 K. [c] Spectra taken at room temperature.

Scheme II

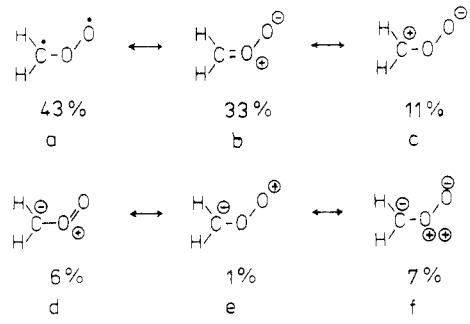

In this work we have tested a variety of semiempirical methods to find an economic but also reasonably reliable quantum chemical treatment for carbonyl oxides with relatively large organic substituents. We have found this method to be MINDO/3-UHF,[13,14] which we have used to calculate ground-state properties of a variety of substituted carbonyl oxides. Results of these calculations have laid a basis for the distinction of the effects of π-donor and π-acceptor substituents on the electronic nature of 1. A classification of carbonyl oxides has been achieved, which has been used to interpret MINDO/3-UHF calculations on carbonyl oxides of spectroscopic interest. For the latter compounds, UV-vis spectra have been calculated with CNDO/S[15] and compared with the available spectroscopic evidence on carbonyl oxides.

Computational Methods

Ab initio calculations at the RHF level of theory exaggerate the zwitterionic character of 1. They lead to a rather short CO bond (ca. 1.2 Å) and a long, very weak OO bond (ca. 1.6 Å) whereby this trend is particularly pronounced for the commonly used split-valence basis sets.[16] A better description of 1 is obtained at the MP level of theory, which predicts similar heavy-atom bond lengths for 1.[8] The most accurate ab initio result presently available has been obtained with fourth-order MP theory. It suggests that the OO bond is slightly longer (1.33 Å, Table II) than the CO bond (1.27 Å).[8c]

Table II. Calculated Bond Lengths and Bond Angles of Formaldehyde Oxide (1)[a]

parameter	MINDO/3 RHF	MINDO/3[b] 2 × 2 CI	MINDO/3 UHF	MP2[c] 6-31G(d)	MP4[d]
R(OO)	1.300	1.268	1.269	1.295	1.329
R(CO)	1.230	1.252	1.281	1.297	1.274
$R(CH_x)$	1.110	1.110	1.104	1.083	1.086
$R(CH_y)$	1.108	1.110	1.104	1.079	1.083
∠COO	125.5	125.7	124.0	120.3	119.2
$\angle H_xCO$	129.4	129.5	128.2	118.0	118.6
$\angle H_yCO$	116.1	116.1	114.8	114.3	115.3
$\Delta H_f°$	22.7	15.8	21.2		
μ	4.16	3.54	2.97	3.47	

[a] Bond lengths R in Å, bond angles in deg, heat of formation $\Delta H_f°$ in kcal mol^{-1}, dipole moment μ in debye. H_x denotes the hydrogen atom in the syn position, H_y the one in the anti position. [b] Reference 11. [c] Reference 8a. [d] Reference 8b.

Semiempirical methods are parametrized to compensate for errors arising from the use of minimal basis sets and from a simplified description of the correlated motions of the electrons within the RHF approach. However, most semiempirical methods fail to provide a reasonable geometry for 1. CNDO- and MNDO-based methods employed in this work (CNDO/2,[17] and MNDO,[18] MNDO 2 × 2 CI,[18] MNDOC,[19] MNDOC with perturbation corrections,[19] AM1[20]) severely underestimate the OO bond length (by 0.1 Å), suggesting a geometry reminiscent of a complex between O_2 and carbene. This description of 1 is completely different from the HF ab initio results and indicates shortcomings of the method and/or insufficient parametrization rather than a HF-dependent exaggeration of zwitterionic character.

The only semiempirical method that leads to a geometry of 1 not too far from the MP4 result[8c] is MINDO/3.[13] Probably, this is due to the fact that MINDO/3 is extensively parametrized.[21] On the other hand, MINDO/3 exaggerates the zwitterionic character of 1, which becomes apparent from the calculated atomic charges and a relatively large dipole moment of 4.16 D (Table II), close to that expected for a zwitterion (ca. 5 D[22]). Obviously, one has to go beyond the RHF approach even at the semiempirical level to get a reasonable description of the biradical character of 1. Hull[11] has done this by including 2 × 2 CI into the MINDO/3 description of 1. He obtained a reasonable geometry and dipole moment for 1 as is shown in Table II.

A much simpler way to improve the semiempirical description of 1 is to use UHF rather than RHF.[9] The RHF wave function of 1 is unstable, i.e., a lower energy is obtained for 1 when α- and β-spin orbitals are optimized separately. In this way, the LUMO of 1, which is an OO and CO antibonding π MO, mixes into the wave function, and as a consequence, the α-HOMO becomes CO antibonding and OO bonding while the β-HOMO adopts a form similar to that of the RHF HOMO. Compared to the RHF heavy-atom bonds, the CO bond becomes longer and the OO bond shorter due to the decoupling of α- and β-electrons at the UHF level. Table II shows that the two

(13) Bingham, R. C.; Dewar, M. J. S.; Lo, D. H. *J. Am. Chem.* **1975**, *97*, 1285.
(14) Bischof, P. *J. Am. Chem. Soc.* **1976**, *98*, 6844.
(15) (a) Del Bene, J. E.; Jaffe, H. H. *J. Chem. Phys.* **1968**, *48*, 1807. (b) Baumann, H. F. *QCPE 333*; Bloomington, IN, 1975.
(16) Cremer, D., unpublished results.
(17) Pople, J. A.; Beveridge, D. L. *Approximate Molecular Orbital Theory*; McGraw-Hill: New York, 1970.
(18) Dewar, M. J. S.; Thiel, W. *J. Am. Chem. Soc.* **1977**, *99*, 4899.
(19) Thiel, W. *J. Am. Chem. Soc.* **1981**, *103*, 1413.
(20) Dewar, M. J. S.; Zoebisch, E. G.; Healy, E. F.; Stewart, J. J. P. *J. Am. Chem. Soc.* **1985**, *107*, 3902.
(21) In this connection, it seems to be important that each bond type is individually parametrized by scaling of the resonance integrals by a parameter β, which is characteristic of the atoms bonded. MNDO, however, uses atom- rather than bond-based scaling parameters β to reduce the number of empirical parameters.
(22) Fessenden, R. W.; Scaiano, J. C. *Chem. Phys. Lett.* **1985**, *117*, 103.

Table III. Ground-State Properties of Substituted Carbonyl Oxides Calculated by MINDO/3[a]

X	Y	R(OO)	R(CO)	∠COO	atomic charges C(1)	O(1)	O(2)	$\Delta H_f°$	μ
				MINDO/3-UHF					
H	H	1.281	1.269	124.0	0.074	0.184	−0.331	21.2	2.97
H	CHO	1.273	1.295	123.5	−0.436	0.592	0.002	−25.3	2.64
H	CH_3	1.281	1.286	123.7	0.096	0.146	−0.315	−0.6	3.13
CH_3	H	1.282	1.289	124.0	0.101	0.114	−0.322	−0.4	3.01
CH_3	CH_3	1.281	1.306	124.4	0.106	0.107	−0.304	−14.9	3.06
NH_2[b]	H	1.284	1.290	124.9	0.175	0.111	−0.330	5.5	2.19
F	H	1.276	1.249	137.8	0.649	0.017	−0.205	−41.0	2.31
F	F	1.294	1.270	132.6	1.015	−0.123	−0.111	−115.2	0.78
				MINDO/3-RHF					
H	H	1.300	1.229	125.4	0.199	0.217	−0.457	22.7	4.17
H	CHO	1.277	1.245	127.0	−0.249	0.596	0.016	−19.9	3.05
CH_3	H	1.301	1.240	125.6	0.222	0.182	−0.462	1.7	4.74
H	CH_3	1.303	1.240	124.9	0.227	0.179	−0.469	1.9	4.40
CH_3	CH_3	1.302	1.254	125.7	0.220	0.152	−0.468	−11.4	4.71
NH_2[b]	H	1.308	1.243	125.6	0.325	0.141	−0.479	7.3	3.53
NH_2[c]	H	1.325	1.266	122.8	0.377	0.061	−0.522	−3.3	6.25
OH	H	1.322	1.255	126.1	0.586	0.057	−0.500	−35.7	3.90
F	H	1.304	1.218	130.4	0.689	0.104	−0.431	−36.3	4.12
F	F	1.301	1.262	121.1	1.091	−0.003	−0.342	−99.0	1.64

[a] Bond lengths R in Å, bond angles in deg, charges q in electrons, heats of formation $\Delta H_f°$ in kcal mol^{-1}, and dipole moments in debye. The substituent X (Y) is in the syn (anti) position. Only staggered conformations have been considered. [b] N sp^3 hybridized. [c] N sp^2 hybridized.

bond lengths are almost equal. The admixture of the LUMO also leads to an improved description of charge distribution and dipole moment. The calculated dipole moment of 2.97 D (Table II) is close to both the MP2 value of 3.47 D and the dipole moments found for peroxy radicals (typically 2.4 D[23]).

A comparison of the various MINDO/3 results listed in Table II reveals that UHF geometry is closest to the MP geometries also shown in Table II. Similar observations have been made when the UHF method has been applied at the ab initio level of theory for 1,3-dipolar species with potential biradical character.[9,24] Hence, MINDO/3-UHF provides a "cheap" alternative for obtaining geometries and other ground-state properties of substituted carbonyl oxides, which are too large to be calculated with correlation-corrected ab initio methods such as MP2 or MP4.[25]

However, when UHF is used, the resulting wave function is contaminated by higher spin states.[26] For example, the MINDO/3-UHF expectation value of the spin operator S^2 is 0.50 for the singlet ground state of 1 while the correct value should be 0. Hence, the singlet wave function is contaminated by triplet (expectation value of S^2: 2.0) and higher spin states. This has to be born in mind when comparing UHF with RHF results.

We have used MINDO/3-UHF to obtain enthalpies, geometries, and dipole moments for a number of substituted carbonyl oxides. In addition, we have calculated electron density, charge density, and spin density distributions with the MINDO/3-UHF approach. For some selected cases, three-dimensional displays of these functions have been generated at a constant electron density value of 0.002 au (Figures 1–4) with the program package MOLEK-9000.[27] Francl and co-workers have shown that these surfaces envelop atomic volumes compatible with average van der Waals radii.[28]

The charge density is defined as the negative difference density, which is obtained as the difference between the molecular electron density distribution and a superposition of the isotropically averaged electron density distributions of the isolated atoms in their ground state fixed at the geometrical positions they would take in the molecule. The spin density distribution is the difference between the α-electron density and the β-electron density distributions. Calculating a spin-polarized singlet state calls for breaking the spin symmetry which otherwise would lead to the RHF result. This is achieved by randomly changing the α-spin bond order matrix in the first SCF cycle.

The CNDO/S method by Del Bene and Jaffe,[15] which is known to reproduce UV–vis transitions of both $\pi \rightarrow \pi^*$ and $n \rightarrow \pi^*$ types, has been used to calculate the spectra of carbonyl oxides that are of experimental interest. For these calculations, MINDO/3-UHF geometries have been used throughout. The seven highest occupied and the seven lowest unoccupied molecular orbitals have been considered when constructing singly and doubly excited configurations. The energy of the CI states was restricted to 15 eV.

Results and Discussion

Tables III and IV contain geometrical data, atomic charges, enthalpies, and dipole moments of substituted carbonyl oxides calculated with the MINDO/3 method. For reasons of comparison, both RHF and UHF results are given in Table III. Since the geometry of the COO entity is of major concern only distances R(OO) and R(CO) as well as the COO angle are listed.[29] Table V summarizes π populations and spin densities for some selected carbonyl oxides. Calculated UV–vis transitions can be found in Table VI.

The Electronic Structure of Carbonyl Oxide. The electronic structure of 1 is best described by the resonance structures a–f shown in Scheme II, which also gives the

(23) Fessenden, R. W.; Hitachi, A.; Ngarajan, V. *J. Phys. Chem.* **1984**, *88*, 107.
(24) Kahn, S. D.; Hehre, W. J.; Pople, J. A. *J. Am. Chem. Soc.* **1987**, *109*, 1871.
(25) In this connection, it is interesting to note that UHF calculations at the MNDO, MNDOC, and AM1 level of theory lead to deterioration rather than an improvement of the geometry of 1.
(26) See, E.g.: Szabo, A.; Ostlund, N. S. *Modern Quantum Chemistry, Introduction to Advanced Electronic Structure Theory*; MacMillan Publishing Co.: New York, 1982.
(27) Program package MOLEK-9000 developed by P. Bischof, Universität Heidelberg, and by ISKA, Bensheim.
(28) Francl, M. M.; Hout, R. F., Jr.; Hehre, W. J. *J. Am. Chem. Soc.* **1984**, *106*, 563.
(29) RHF and UHF geometries are available from the authors.

Table IV. Some Ground-State Properties of Carbonyl Oxides Calculated by MINDO/3-UHF[a]

carbonyl oxides	R(CO)	R(OO)	∠COO	atomic charges C(1)	atomic charges O(1)	atomic charges O(2)	X_{SO}
1	1.269	1.281	124.0	0.074	0.183	−0.331	(0.94)[b]
2a (syn)	1.298	1.279	125.2	0.113	0.118	−0.296	
2b (anti)	1.300	1.280	122.7	0.112	0.115	−0.285	
5	1.313	1.280	124.9	0.124	0.087	−0.298	0.83
9	1.305	1.280	122.9	0.203	0.084	−0.256	0.87
11	1.305	1.280	124.0	0.150	0.090	−0.281	0.93
13	1.325	1.278	123.0	0.167	0.069	−0.232	(0.61)[c]
15	1.329	1.279	123.9	0.127	0.071	−0.273	
16	1.321	1.277	130.0	0.126	0.065	−0.285	1.00
17	1.348	1.293	125.5	0.769	−0.056	−0.282	

[a] Bond lengths R in Å, angles in deg, and atomic charges in electrons. X_{SO} measures the nucleophilicity of oxidizing reagents. The largest value is 1.0. See ref 32 for definition and values. [b] *tert*-Butyl carbonyl oxide, ref 32. [c] Naphthoquinone oxide, ref 32.

Table V. pπ Populations and Spin Densities of Substituted Carbonyl Oxides Obtained with MINDO/3-UHF

X	Y	pπ populations C(1)	pπ populations O(1)	pπ populations O(2)	N_π[a]	pπ spin densities[b] C(1)	pπ spin densities[b] O(1)	pπ spin densities[b] O(2)
H	H	0.990	1.444	1.566	4.000	0.653	−0.253	−0.400
H	CHO	1.022	1.469	1.438	3.929	0.656	−0.221	−0.523
CH_3	H	1.007	1.471	1.534	4.012	0.657	−0.264	−0.436
CH_3	CH_3	1.021	1.493	1.500	4.014	0.668	−0.273	−0.474
F	H	0.495	1.692	1.954	4.141	0.072	−0.061	−0.018
F	F	0.438	1.786	1.978	4.202	0.044	−0.034	−0.008

π-conjugated carbonyl oxides	pπ populations C(1)	pπ populations O(1)	pπ populations O(2)	N_π[a]	pπ spin densities[b] C(1)	pπ spin densities[b] O(1)	pπ spin densities[b] O(2)
2a	1.014	1.503	1.489	4.006	0.619	−0.285	−0.491
5	1.015	1.508	1.481	4.004	0.640	−0.289	−0.497
9	0.944	1.522	1.428	3.894	0.561	−0.264	−0.552
13	0.973	1.552	1.403	3.928	0.528	−0.278	−0.582
15	1.040	1.546	1.452	4.038	0.549	−0.312	−0.536
17	0.499	1.803	1.974	4.276	0.026	−0.015	−0.006

[a] Number of π-electrons. [b] Negative (positive) values denote an excess of α(β)-spin density.

Table VI. UV-Vis Transitions of Carbonyl Oxides Calculated with the CNDO/S Method Using MINDO/3-UHF Geometries[a]

carbonyl oxide	$\pi \rightarrow \pi^*$[b]	$n \rightarrow \pi^*$[c]	other transitions[d]
1	384 (3.77)	774 (1.60)	165 (3.30), 133 (2.57)
2a (syn)	423 (3.98)	598 (1.34)	304 (2.51), 243 (3.00)
2b (anti)	427 (4.09)	598 (1.52)	304 (2.34), 243 (2.99)
5	455 (3.84)	648 (1.60)	298 (3.29), 283 (2.40)
9	424 (4.03)	784 (1.00)	570 (1.64), 296 (2.47)
11	489 (3.98)	765 (1.01)	416 (2.36), 308 (1.94)
13	468 (4.10)	859 (1.10)	362 (2.12), 265 (3.18)
15	546 (3.99)	703 (1.40)	672 (2.10), 271 (0.92)
16	493 (3.87)	754 (0.39)	439 (2.70), 346 (3.21)
17	504 (3.72)	768 (1.73)	166 (3.39), 143 (2.97)

[a] Transitions in nm. Intensities given as log ε in parentheses. [b] Polarization in the COO plane. [c] Polarization out of the COO plane. [d] Only the two most intense transitions are given. These are $n \rightarrow \pi^*$ (165 nm) and $\pi \rightarrow \pi^*$ (133 nm) transitions in the case of 1. In the other cases, they correspond to $\pi \rightarrow \pi^*$ transitions involving π MOs of the substituents (exception: 17, 143 nm, $n \rightarrow \pi^*$ transition).

weights of the six resonance structures in a nonempirical valence bond wave function of 1.[30] The biradical structure a should dominate the wave function. The calculated weight of 43% is probably still too low.[30] Resonance structure b is in line with the denotation of 1 as formaldehyde oxide. Its weight (33%, Scheme II) is overestimated in the same way as the one of b is underestimated. The other resonance structures c–f contribute less than either a or b to the ground-state wave function of 1, but they may gain importance for substituted 1.

(30) Hiberty, P. C. *Isr. J. Chem.* **1983**, *23*, 10.

The MINDO/3-UHF description of 1 clearly supports the biradical character of the molecule. This can be seen from Figures 1 and 2, which depict colored three-dimensional displays of the charge density (Figure 1) and the spin electron density distribution of 1 (Figure 2) calculated at a constant electron density value of 0.002 au. Both the largest positive and the largest negative charge density are found in the σ-plane at O(2) (white-blue and red area in Figure 1). This is in line with the description of the electronic structure given by resonance formula b. The semipolar O(1)–O(2) bond involving the in-plane electron lone pair at O(1) pushes electron density at O(2) out of the direction of the σ-bond axis into the region of the electron lone pair at O(2). However, it must be remembered that this effect is exaggerated by the charge density distribution due to comparison with an artificial reference state, the isotropically averaged electron density of $O(^3P)$. Averaging increases the electron density in the singly occupied 2p orbitals, but decreases it in the doubly occupied 2p orbital. As a consequence, there always seems to be a decrease (increase) of electron density in the direction of the σ-bond (in the region of the lone pair) when the O atom is incorporated in a molecule. In any case, the charge density distribution shown in Figure 1 suggests that the electron distribution of O(2) entails both nucleophilic and electrophilic character for 1.

Negative charge densities are found in the π regions at C(1) and at O(2) (yellow areas in Figure 1). This is in line with the biradical resonance structure a, in which the terminal O atom donates one of its two π-electrons (e.g., that pushed out of the σ direction) to the CO unit, thus canceling largely the positive charge at O(1) (there is green rather than blue at O(1); see Figure 1). Hence, O(2) withdraws σ-density and back-donates π-density to O(1),

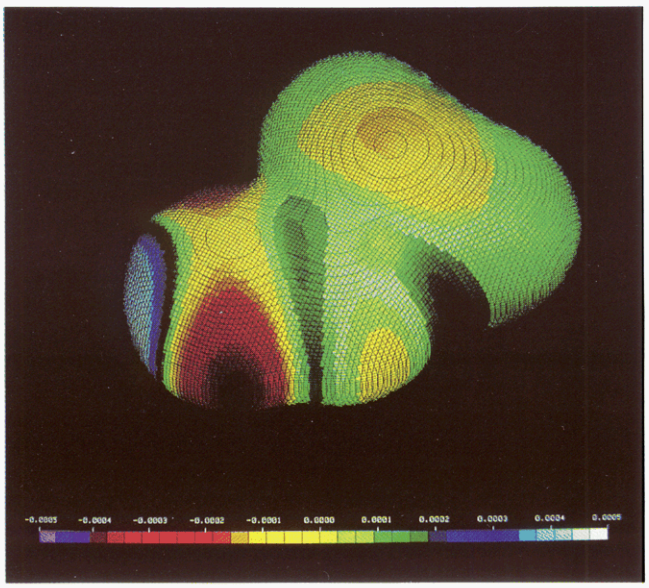

Figure 1. Perspective drawing of the valence charge density distribution of formaldehyde oxide (**1**). The valence charge density is given for a constant value of the valence electron density distribution (0.002 au). Negative values are red-violet, positive values blue (see scale).

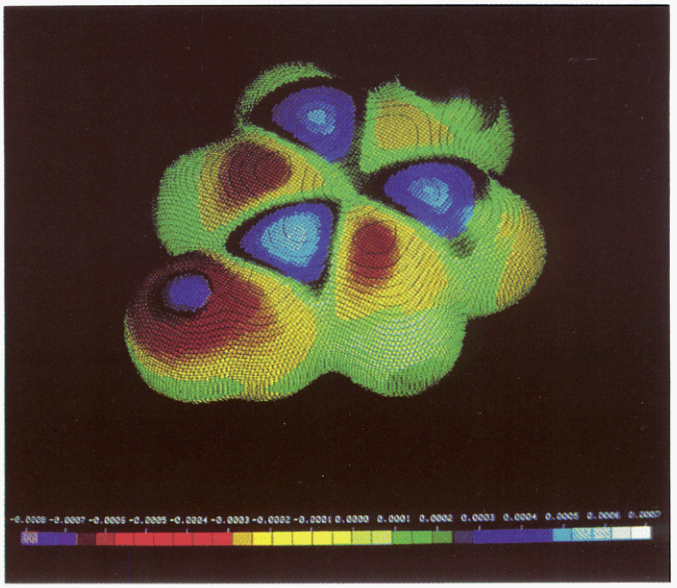

Figure 3. Perspective drawing of the valence charge density distribution of quinone oxide (**13**). The valence charge density is given for a constant value of the valence electron density distribution (0.002 au). Negative values are red-violet, positive values blue (see scale).

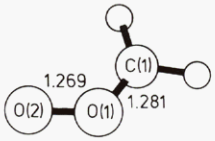

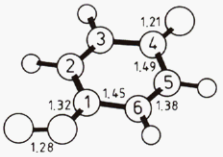

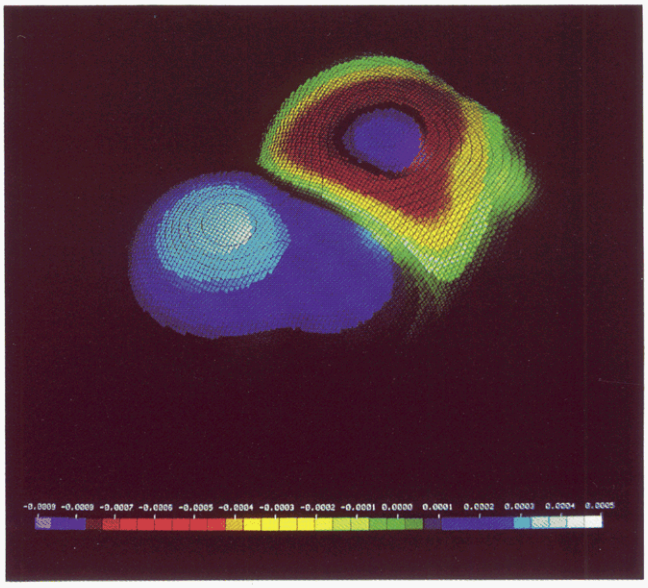

Figure 2. Perspective drawing of the valence spin density distribution of formaldehyde oxide (**1**). The valence spin density has been calculated for a constant value of the valence electron density distribution (0.002 au). Excess α-spin density is given in red-violet, excess β-spin density in blue. Molecular regions without spin polarization are given in green (see scale).

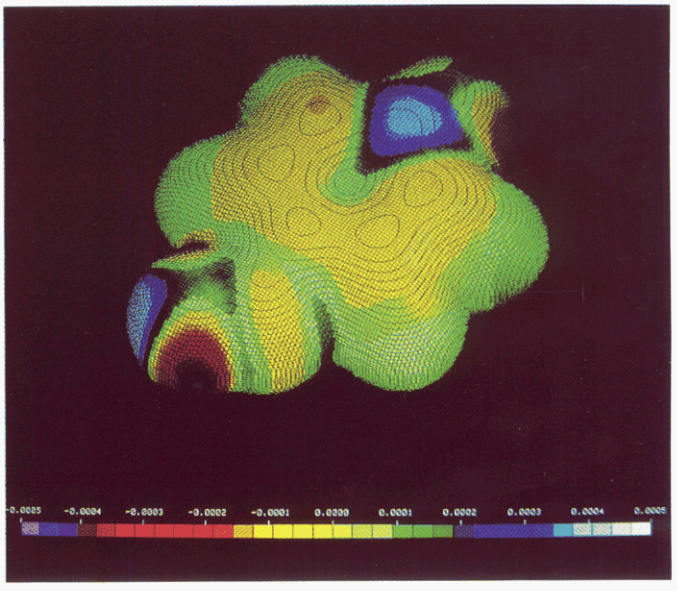

Figure 4. Perspective drawing of the valence spin density distribution of quinone oxide (**13**). The valence spin density has been calculated for a constant value of the valence electron density distribution (0.002 au). Excess α-spin density is given in red-violet, excess β-spin density in blue. Molecular regions without spin polarization are given in green (see scale).

thereby establishing a fairly strong OO bond. The full extent of π-back-donation is only described by methods including correlation corrections or by decoupling of electron pairs as in the UHF approach.

The biradical character of 1 can also be assessed from the spin density distribution given in Figure 2. The π-system of 1 as described by MINDO/3-UHF is highly spin polarized (white and purple regions in Figure 2) while the σ-system contains the same densities of α- and β-electrons. At O(2), there is an excess of 0.40 π-electrons with α-spin, O(1) carries a small excess of 0.25 π-electrons, and C(1) possesses a surplus of 0.65 electrons with β-spin (Table V). Again, this agrees with the description of 1 as a singlet 1,3-π-biradical.[7-10] Although there is no experimental proof for this spin distribution, the radical-like character of carbonyl oxides is suggested by observed hydrogen abstraction and autoxidation via radical chain reactions.[12]

Influence of π-Acceptor and π-Donor Substituents. For some substituted 1, MINDO/3-UHF also leads to a lower heat of formation than MINDO/3-RHF, indicating that the biradical character of 1 is largely preserved upon substitution (see Table III). However, for other substituents, it is no longer possible to obtain a UHF wave function, probably because of a significant change in the electronic structure of the carbonyl oxide. To assess these changes, we have listed in Table III both UHF and RHF results for substituted 1.

Table III reveals that a π-acceptor substituent such as CHO leads to a decrease of the OO bond length and to an increase of the CO bond length with the result that R(OO) < R(CO). The calculated charges given in Tables III and V indicate that negative charge, predominantly π-charge, is transferred from the two O atoms to the C atom as in resonance structures d–f. A π-acceptor gives more weight to these resonance structures, which all furnish the C atom of 1 with a formal negative charge. In this way, negative charge can delocalize onto the substituent, thus leading to an overall stabilization of the molecule. A CHO substituent withdraws 71 me from the 4π system of 1. It is interesting to note that spin polarization and, hence, biradical character of 1 are maintained upon substitution by the π-acceptor substituent CHO (Table V).

Increased importance of resonance structures d–f will lead to typical changes in the heavy-atom bonds. The OO bond becomes shorter (due to an OO double bond in d, reduced pπ,pπ repulsion in e, and increased electrostatic attraction between the O atoms in f), and the CO bond lengthens (due to increased CO single-bond character in d–f). This is in line with the MINDO/3 results for CHO-substituted 1 (Table III).

A π-donor substituent should cause a transfer of π charge from the C atom to the O atoms as in the 1,3-dipolar structure c (Scheme II). An increased weight of structure c, in turn, leads to lengthening of both the CO bond (due to increased single-bond character) and the OO bond (due to increased pπ,pπ repulsion). The calculated geometries and atomic charges of π-donor-substituted derivatives of 1 given in Table III fully confirm these predictions.

A substituent such as methyl donates π-density (ca. 10 me, Table V) into the π-system of 1 via hyperconjugative interactions. There is a distinct lengthening of the CO bond by 0.02 Å while the donor effect of methyl obviously does not suffice to increase the OO bond length (Table III). The calculated charges and the spin densities at C(1) and O(2) (see Table V) clearly indicate that the biradical character of 1 is not affected by methyl substitution. Similar geometries, charges, and spin densities can be found when the second H of 1 is replaced by another methyl group or CH_3 is replaced by an (sp^3-hybridized) NH_2 group (Table III).

Contrary to ab initio calculations, which clearly predict *syn*-methyl-substituted 1 to be more stable than *anti*-methyl-substituted 1 due to the cis effect,[8a] MINDO/3 fails to describe this effect properly (Table II). Since the cis effect is also active for other substituted carbonyl oxides,[8c] we will consider in the following discussion only syn derivatives of 1.

A π-donor substituent such as OH or sp^2-hybridized NH_2 has a stronger impact on the electronic structure of 1, as is clearly revealed by the fact that an UHF wave function is no longer obtained for these derivatives. Comparison of the RHF geometries also shown in Table III reveals that the OO and CO bond lengths are both increased by 0.02–0.03 Å, reflecting the importance of resonance structure c and, hence, increased zwitterionic character of π-donor-substituted 1.

So far, we have assumed that the substituent primarily influences the easily polarizable 4π system of 1 rather than the σ framework. This, however, is no longer true for a strongly electronegative substituent such as F, which is a distinct σ-acceptor, but a weak π-donor. F is known to lead to a significant shortening of adjacent heavy-atom bonds,[31] and this effect is also reflected by the CO bond of F-substituted 1. MINDO/3 suggests also a slight decrease of the OO bond length, in clear disagreement with the more reliable ab initio results, which predict lengthening of the OO bond by 0.04 Å.[8c] It is noteworthy that a F substituent, although a weaker π-donor than either OH or sp^2-hybridized NH_2, leads to a substantial reduction of the biradical character, as is indicated by the calculated spin densities (Table V). This applies also to difluoro-substituted 1 (Table V).

From the MINDO/3 calculations, the following conclusions can be drawn.

1. A π-acceptor substituent leads to a shortening of the OO bond and a lengthening of the CO bond. π-Density is transferred from the COO unit to the substituent. Resonance structures d–f become more important.

2. A π-donor substituent leads to a lengthening of both the OO and the CO bond. π-Density is transferred from the substituent to C and the O atoms. Resonance structure c becomes more important.

3. If the substituent is also a strong σ-acceptor (σ-donor), σ-effects superpose the π-effects. For example, F leads to a shortening of the CO bond despite its π-donating property.

4. Since the electron impact of the substituent is stronger for the C than the O atoms, changes in the CO bond length are somewhat larger (0.06 Å) than those in the OO bond lengths (0.04 Å). Calculated bond lengths range from 1.27 to 1.31 Å (OO bond) and from 1.25 to 1.31 Å (CO bond), i.e., they are all close to the OO bond in ozone (1.278 Å), which is isoelectronic with 1. There is a distinct correlation between the energy of the LUMO and the length of the OO and CO bonds. The lower the energy of the LUMO is, the longer become the heavy-atom bonds.

5. The calculated spin densities suggest that the biradical character of 1 is preserved if the substituent is a weak π-donor or π-acceptor. For example, alkyl substituents, which influence the electronic structure of 1 by hyperconjugative interactions, do not change the electronic nature of 1 significantly.

It will be interesting to see whether these conclusions also apply to carbonyl oxides with large organic substituents and which have been or can be spectroscopically

(31) Yokozeki, A.; Bauer, S. H. *Top. Curr. Chem.* **1975**, *53*, 71.

characterized by the techniques mentioned in the introduction. Therefore, we will extend our investigation of substituent effects in the next section.

π-Conjugated Carbonyl Oxides. UHF calculations of phenyl-substituted carbonyl oxides **2** (**2a** = *syn*-**2**, **2b** = *anti*-**2**) and **5**, the cyclopentadienone oxides **15** and **16**, quinone oxide **13**, and the tropone oxides **15** and **16** (Scheme I) all yield a wave function typical of a molecule with large 1,3-biradical character (see spin densities in Table V). A conjugated system adjacent to the COO unit leads to delocalization of both π-electrons and spin density. This is nicely reflected by Figures 3 and 4, which show colored three-dimensional displays of charge and spin density distribution of quinone oxide **13**. Figure 3 shows that both C(1) and O(2) of the COO unit are no longer as negatively charged as in the parent compound (see Figure 1). This is in line with increased π-back-donation from O(2) to O(1) and π-delocalization into the quinone π-system, which functions as a π-acceptor (see N_π in Table V). The fact that **13** possesses the highest OO vibrational frequency of all carbonyl oxides for which infrared data are available[2b] suggests OO bond strengthening due to enhanced π-back-donation, although the calculated OO bond length for **13** does not reflect this (Table IV).

Figure 3 also reveals that the carbonyl carbon is strongly positively charged (blue-white area in π direction), which is in line with the pronounced π-withdrawing ability of the carbonyl group. (Note that the negative charge of the carbonyl oxygen cannot be seen in the charge density distribution due to the artifacts described above.) Obviously charge polarization is smaller in the COO group than in the carbonyl group. When charge polarization within the COO group is compared, calculated atomic charges (Table IV) clearly show that charge polarization is larger in the OO bond than in the CO bond. This can also be deduced from the relative intensities of the CO and OO stretching frequencies either calculated at the MP2[8b] level or taken from the experimentally available infrared spectra. In almost all carbonyl oxides investigated so far, the OO stretching mode is the most intense band in the spectrum while the CO stretching mode is barely detectable.[1-3] Figure 4 shows that excess spin is delocalized into the π-system of the six-membered ring of **13**, α-spin from C(1) to the meta C atoms (blue regions) and β-spin to the ortho and para C atoms (red and yellow regions in Figure 4).

The carbonyl oxides listed in Table IV can be divided into three groups, the first of which comprises **2a**, **2b**, and **5**. The phenyl substituents affect carbonyl oxide by extending its π-system and donating some π-density to carbonyl oxide, thus lengthening both the CO and OO bonds. in the second group are the ring carbonyl oxides **9**, **11**, and **13**. As already discussed for **13**, the ring functions as a π-acceptor. In this way, **9** and **11** (as well as **10** and **12**) adopt an electron structure in their ring portion that is closer to the energetically favorable electron sextet of the cyclopentadienyl anion. The calculated CO bond lengths reflect the electron-withdrawing effect of the ring, but the OO bond lengths do not show the changes found for a strong π-acceptor such as the aldehyde group.

Compounds **15**–**17** form the third group of carbonyl oxides investigated. In **15** and **16**, the ring acts as a π-donor to come closer to the stable π-configuration of the tropylium cation. In **17**, C(1) is linked to two O atoms, which donate π-density into the COO unit. Calculated charges and geometries are in line with the predictions made for π-donor-substituted **1** in the previous section.

Carbonyl oxide **17** is the only compound that possesses increased zwitterionic character as indicated by the calculated spin densities (Table V). We conclude that organic substituents with another C atom directly attached to C(1) do not change the electronic structure of **1** dramatically. Of course, solvent effects can lead to zwitterionic character, as has been suggested previously.[7]

We have compared calculated charge densities q at O(2) with the relative nucleophilicities of carbonyl oxides measured by Adam and co-workers.[32] These authors have established the X_{SO} scale, which gives the ratio of sulfoxide vs sulfide attack obtained from reactions of thianthrene 5-oxide with a nucleophile. Exclusive nucleophilic oxidation corresponds to $X_{SO} = 1$. Since carbonyl oxides are basically nucleophilic, X_{SO} is found to be in the range from 1 to 0.6 (see Table IV). There is some correlation between the known X_{SO} values of **9**, **11**, **13**, and **16** in the way that the more negatively charged O(2) atom corresponds to a higher value of X_{SO}. In other words, π-donor substituents increase, π-acceptor substituents decrease the nucleophilicity of carbonyl oxides. It seems that alkyl and aryl substituents, which are weak π-donors and which may act not only electronically but also sterically, do not fit in this correlation (see the X_{SO} value for **5**). However, more experimental data are needed to confirm this.

Substituent Effects on the UV–Vis Spectra

Since 1984 a number of UV–vis spectra of carbonyl oxides have been reported in the literature (Table I). All spectra have very strong and broad bands in the visible region (380–460 nm). In some cases these bands exhibit vibrational fine structure. By using ^{18}O isotopic labeling it was shown that in **3** the fine structure is caused by the O–O stretching vibration of the carbonyl oxide moiety.[2b] Matrix-isolated carbonyl oxides are intense yellow or orange.[1-3]

MINDO/3-UHF optimized geometries were used to calculate UV–vis transitions with the CNDO/S method. The inclusion of doubly excited configurations not only affects the excited states of carbonyl oxides, but also leads to a significant depression of the ground-state energies. This again shows that carbonyl oxides possess biradical character and treatment as a closed shell molecule is inadequate.

The CNDO/S-calculated UV–vis transitions of carbonyl oxides are summarized in Table VI. These calculations predict two transitions characteristic for the carbonyl oxide functional group, namely, a very strong $\pi \rightarrow \pi^*$ transition and a weak $n \rightarrow \pi^*$ transition.

The $\pi \rightarrow \pi^*$ transitions are calculated to be the strongest transitions in the spectra of carbonyl oxides ($\log \epsilon \approx 4$), localized between 384 and 546 nm (Table VI). The polarization of these bands is parallel to the COO plane. The high intensity and the easily accessible spectra region make the $\pi \rightarrow \pi^*$ transition most important for the identification and characterization of carbonyl oxides.

A comparison with the data given in Table I shows the excellent agreement between calculated transitions and the maxima of the most intense bands found in matrix isolation studies or laser flash photolysis experiments (the exact 0–0 transitions are generally not available). In all cases where experimental data are available, the calculated transitions lie within the observed bands. The largest deviation between calculated transitions and experimental maxima is found for benzophenone oxide **5** (33 nm).

The position of the calculated $\pi \rightarrow \pi^*$ transition depends on the geometry used in the CNDO/S calculations. For

(32) Adam, W.; Dürr, H.; Haas, W.; Lohray, B. *Angew. Chem.* **1986**, *98*, 85; *Angew. Chem., Int. Ed. Engl.* **1986**, *101*.

compound 1, the transition is shifted from 384 to 376 nm if the MINDO/3-RHF instead of UHF optimized geometry (Table II) is used.

The position of the $\pi \rightarrow \pi^*$ transition depends on the size of the π-system and the π-electron donating or withdrawing capabilities of substituents. Large, conjugated π-systems as in **9**, **11**, **13**, **15**, and **16** cause red shifts compared to **1**. A large red shift is also calculated for **17**, which has the smallest π-system (besides **1**) but the highest electron density in the π-system (Table V). Thus π-electron-donating groups lead to red shifts of the $\pi \rightarrow \pi^*$ transitions. The opposite effect was found for electron-withdrawing groups: in trifluoroacetophenone *O*-oxide, the band is blue-shifted to 378 nm, which is the lowest value observed, so far. (Since MINDO/3 does not give reasonable geometries for compounds containing CF_3 groups, no calculations have been performed.)

The influence of π-systems can also be seen by comparison of **9** and **15** with their bis-benzo-annellated derivatives **11** and **16**. The π-electron-donating capability of the tropylidene moiety in **15** causes a red shift (compared to **1**) of 162 nm. The π-electron-withdrawing cyclopentadienylidene group in **9** leads only to a red shift of 40 nm. Benzo annellation has the opposite effect on the spectra of **9** and **15**: the calculated transitions in **11** and **16** are at 489 and 493 nm, respectively, and thus the spectrum of **11** is red-shifted while the spectrum of **16** is blue-shifted (compared to the parent compounds **9** and **15**). The larger π-systems lead to better charge delocalization, and therefore the influence on the charge density in the COO group is diminished.

The $n \rightarrow \pi^*$ transitions of carbonyl oxides are calculated to occur at long wavelengths in the red part of the spectrum. The very low intensity of these transitions prohibited the direct experimental observation. The only indirect hint comes from the photochemistry of carbonyl oxides. On long-wavelength irradiation ($\lambda > 600$ nm), carbonyl oxides rearrange to give dioxiranes or split off oxygen atoms to give the corresponding carbonyl compounds.[1-3] This photochemistry is explained best by assumption of a low-intensity band above 600 nm.

Conclusion

A comparison of the results of semiempirical calculations and experimental data demonstrates the importance of substituents on the properties of carbonyl oxides. The largest influence comes from substituents changing the charge density of the four-electron π-system of the COO moiety. A π-acceptor substituent leads to a shortening of the OO bond and a lengthening of the CO bond. Both heavy-atom bonds are lengthened by the electronic impact of a π-donor substituent. Fluoro substituents, which are both π-donors and strong σ-acceptors, lead to shortening of the CO and lengthening of the OO bond. These trends can be predicted by analyzing the contribution of the various resonance structures to the ground-state wave function of carbonyl oxide. In addition, they explain observed frequencies of the OO stretching vibration or shifts of the π-π^* transitions.

Strong π-donor substituents increase the zwitterionic character of carbonyl oxides while weak π-donors of π-acceptors seem to largely preserve the biradical character of the parent compound.

Changes in the geometry and in the charge distribution of carbonyl oxides upon substitution are important to know when making predictions with regard to the reactivity of these reactive intermediates. π-Donors will increase, π-acceptors will decrease the nucleophilicity of carbonyl oxides. This has been deduced from the calculated charges at O(2) and the correlation between the latter and measured X_{SO} values. Also, a carbonyl oxide with enhanced zwitterionic character will undergo reactions typical of 1,3-dipoles. Eventually, zwitterionic character of carbonyl oxide will facilitate isomerization to dioxirane,[8b] thus showing a different reactivity pattern than the parent carbonyl oxide.

This work shows that MINDO/3-UHF calculations provide a reasonable insight into the ground-state properties of substituted carbonyl oxides while CNDO/S is the method of choice to get information on their electronic transitions. As long as correlation-corrected ab initio calculations on large molecules are prohibitively time consuming, semiempirical descriptions will aid experimental investigations on such elusive species as carbonyl oxides.

Acknowledgment. We thank Prof. R. Gleiter for supporting this work. Financial support was given by ISKA, Bensheim, Hewlett Packard, the Deutsche Forschungsgemeinschaft, and the Fonds der Chemischen Industrie. Calculations have been carried out on a HP 9000 work station and on the CDC CYBER 7600 of the Rechenzentrum der Universität Köln.

Registry No. **1**, 78894-19-6; **2**, 78894-20-9; **5**, 86508-70-5; **9**, 88766-67-0; **11**, 96746-58-6; **13**, 118949-77-2; **15**, 118949-78-3; **16**, 99967-20-1; **17**, 118949-79-4; $OHCC(O_2)H$, 118949-74-9; $H_3CC(O_2)H$, 68941-70-8; $(H_3C)_2CO_2$, 65339-02-8; $H_2NC(O_2)H$, 118949-75-0; $FC(O_2)H$, 112897-49-1; F_2CO_2, 114395-52-7; $HOC(O_2)H$, 118949-76-1.